YbH^+ formation in an ytterbium ion trap

Thai M. Hoang,[1] Yuan-Yu Jau,[1] Richard Overstreet,[2] and Peter D. D. Schwindt[1]
[1]*Sandia National Laboratories, Albuquerque, New Mexico 87123, USA*
[2]*Microchip Technologies, Inc., Beverly, Massachusetts 01915, USA*

(Received 7 August 2019; revised manuscript received 13 January 2020; accepted 21 January 2020; published 14 February 2020)

The trapped $^{171}Yb^+$ ion is a promising candidate for portable atomic clock applications. However, with buffer-gas cooled ytterbium ions, the ions can be pumped into a low-lying $^2F_{7/2}$ state or form YbH^+ molecules. These dark states reduce the fluorescence signal from the ions and can degrade the clock stability. In this work, we study the dynamics of the populations of the $^2F_{7/2}$ state and YbH^+ molecules under different operating conditions of our $^{171}Yb^+$ ion system. Our study indicates that $^2F_{7/2}$-state ions can form YbH^+ molecules through interactions with hydrogen gas. As observed previously, dissociation of YbH^+ is observed at wavelengths around 369 nm. We also demonstrate YbH^+ dissociation using 405 nm light. Moreover, we show that the population in the dark states can be limited by using a single repump laser at 935 nm. Our study provides insights into the molecular formation in a trapped ion system.

DOI: 10.1103/PhysRevA.101.022705

I. INTRODUCTION

The past two decades have witnessed significant efforts in miniaturizing atomic clocks. There are several approaches to miniaturize an atomic clock such as laser-cooled atoms [1–3], vapor-cell atomic clocks [4–7], and trapped ion clocks [8]. We focus on developing a highly miniaturized microwave atomic clock which is operated using the 12.6 GHz hyperfine ground-state transition of trapped $^{171}Yb^+$ ions [9–11]. Previous studies have shown that $^{171}Yb^+$ ions can be pumped in the $^2F_{7/2}$ state [12–20] and form a YbH^+ molecule [21,22]. As a result, the $^{171}Yb^+$ signal can be reduced and the clock stability is degraded. Understanding the $^2F_{7/2}$-state trapping and the YbH^+ molecular formation is one of the keys to the compact $^{171}Yb^+$ atomic clock. In this paper, we investigate the YbH^+ formation of trapped ions.

Previous studies have suggested that YbH^+ molecular ions can be formed from the $^2F_{7/2}$-state or $^2D_{3/2}$-state ions through an interaction with hydrogen gas [21,22]. Since it is difficult to completely remove hydrogen from a vacuum system, the YbH^+ formation can be problematic in a passively pumped vacuum package [9–11,20]. We investigate the YbH^+ formation mechanism under different optical excitation conditions in such a passively pumped package. To optically excite the ions, 369, 405, 760, and 935 nm lasers are used, and microwave radiation drives transitions within the $^2S_{1/2}$ ground state. Primarily, we investigate the YbH^+ dynamics when both the optical and microwave radiation are applied continuously, and we compare our data to a rate-equation model to understand the populations of the various states. We also perform a limited study of the populations when the lasers and microwave radiation are sequentially pulsed, and the rate equation is modified to account for only long-timescale population dynamics. While our results do not rule out the formation of YbH^+ molecules from the $^2D_{3/2}$ state, our results suggest that YbH^+ are formed predominantly from $^2F_{7/2}$-state ions. Dissociation of YbH^+ has previously been observed at wavelengths of 369.48, 369.44, 369.20, and 368.95 nm [14,21,22]. We demonstrate that dissociation can also be achieved using 405 nm light from a free-running edge-emitting diode laser. Moreover, we illustrate that the 935 nm light can sufficiently prevent the molecular formation.

II. EXPERIMENTAL SYSTEM

The experiments are carried out in a 3 cm^3 vacuum package developed and constructed by the Jet Propulsion Laboratory [Fig. 1(b)]. The vacuum package is permanently sealed with a copper pinch-off and passively pumped with a nonevaporable getter. The vacuum package details are described in Refs. [9–11]. The chamber is baked out to achieve 10^{-10} torr level. The vacuum package is backfilled with 4×10^{-6} Torr of neon (as read from an ion gauge without a gas correction factor applied), which provides buffer-gas cooling of the ions. A Yb oven is heated to above 300 Celsius to produce Yb atomic vapor. The Yb atoms are then ionized by electrons produced by the photoelectric effect. To produce an emission of electrons, we shine about 10 mW of the 405 nm laser light onto the Yb-coated trap rods. The $^{171}Yb^+$ ions are trapped in a linear quadrupole rf Paul trap which has 240 V_{rms} applied between adjacent trap rods at 3.35 MHz, and the four trap rods are held at a -20 V potential difference relative to the grounded end-cap electrodes of the trap. Microwave radiation is applied to the ions by coupling the microwave power into the package through the trap rods. A magnetic field of ~230 mG is applied in the perpendicular direction of the laser beam. This magnetic field will result in a Zeeman splitting of ~300 kHz in the $|^2S_{1/2}, F = 1\rangle$ state, while the trapping frequency is typically ~400 kHz. The 935 nm laser (~0.5 mW) is used to clear the low-lying $^2D_{3/2}$ state, and the 760 nm laser (~0.5 mW) is used to clear the $^2F_{7/2}$ state. The 369 nm laser is used for state detection and optical pumping. A 250 mm focal lens is used to focus these laser beams at the

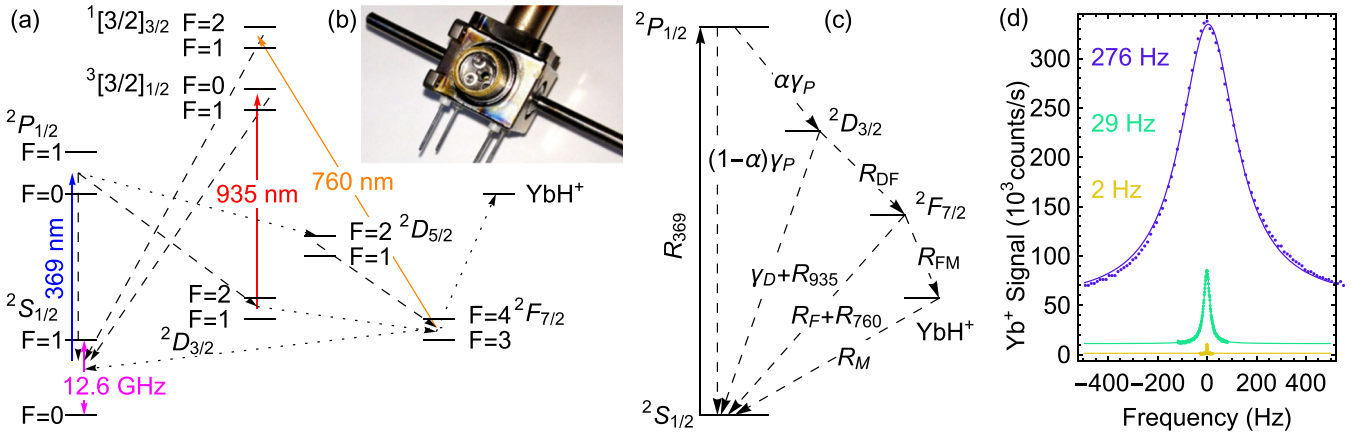

FIG. 1. (a) Simplified energy level diagram of the $^{171}Yb^+$ ion. The solid arrows show the laser transitions. The dashed arrows show the spontaneous decays. The dotted arrows show collisional decays. (b) Photograph of the 3 cm^3 vacuum package. (c) A simplified rate-equation diagram illustrates the levels and the transitions used in the rate-equation model. (d) Microwave linewidth measurements. The data (circle markers) are fitted to the Lorentzian function (solid line). The numbers indicate the full width at half maximum of the fits. Each measurement is represented by a different color.

ion cloud with the beams passing the hollow end caps of the Paul trap. Fluorescence of trapped ions at 369 nm is collected using a photomultiplier tube. The Yb^+ ion signal is detected using the 369 nm fluorescence. All of the lasers are locked to Bristol wavemeters. The 369 nm laser is estimated to have a frequency stability of ∼100 MHz.

III. THEORETICAL MODEL

To understand the YbH^+ formation, we first consider the transitions between different energy levels of a $^{171}Yb^+$ ion under optical excitation [Fig. 1(a)]. Without the hyperfine structure, the energy diagram can be simplified as shown in Fig. 1(c). Assuming that YbH^+ molecular ions are formed from F-state ions, the rate equations can be written as

$$\begin{aligned}
\dot{n}_S &= -R_{369}n_S + (1-\alpha)\gamma_P n_P + (\gamma_D + R_{935})n_D \\
&\quad + (R_F + R_{760})n_F + R_M n_M, \\
\dot{n}_P &= -\gamma_P n_P + R_{369}n_S, \\
\dot{n}_D &= -(\gamma_D + R_{935} + R_{DF})n_D + \alpha\gamma_P n_P, \\
\dot{n}_F &= -(R_F + R_{760})n_F + R_{DF}n_D - R_{FM}n_F, \\
\dot{n}_M &= R_{FM}n_F - R_M n_M. \qquad (1)
\end{aligned}$$

Here, n_S, n_P, n_D, n_F, and n_M are the relative population of the $S_{1/2}$, $P_{1/2}$, $D_{3/2}$, $F_{7/2}$, and YbH^+ states. The branching ratio of the P state to the D state, α, is ∼0.005 [20]. The spontaneous decay of the P state and D state is γ_P (∼10^8 s^{-1}) and γ_D (∼20 s^{-1}), respectively. R_{369} is the effective pumping rate of the whole $S_{1/2}$ state determined by the settings of the 369 nm laser and the 12.6 GHz microwave radiation. The optical pumping rate of the 760 nm and 935 nm lasers is R_{760} (∼10^{-1} s^{-1}) and R_{935} (∼10^3 s^{-1}), respectively. The rates from the $D \to F$, $F \to YbH^+$, $F \to S$, and $YbH^+ \to S$ states are R_{DF}, R_{FM}, R_F, and R_M, respectively.

For much of this study, the clock was operated in a "continuous mode," where the 12.6 GHz microwave radiation and the resonant 369 nm light continuously illuminate the ions. The full width at half maximum of the clock resonance is determined by optical and microwave power broadening,

$$\mathrm{FWHM} = \frac{1}{\pi}\sqrt{\frac{\beta}{2}\Omega^2 + \left(\frac{\Gamma_{369}}{2}\right)^2}, \qquad (2)$$

where Ω is the microwave Rabi frequency, Γ_{369} is the pumping rate of the 369 nm laser from the $|^2S_{1/2}, F=1\rangle$ state to either hyperfine level of the $|^2P_{1/2}\rangle$ state, and β is the average number of photons scattered before optical pumping to the $|^2S_{1/2}, F=0\rangle$ state. For the $|^2S_{1/2}, F=1\rangle$ to $|^2P_{1/2}, F=1\rangle$ (1-to-1 transition), $\beta = 3$, while for the $|^2S_{1/2}, F=1\rangle$ to $|^2P_{1/2}, F=0\rangle$ transition (1-to-0 transition), $\beta =$ 300 to 500, depending on the ion temperature. To obtain the maximum signal (i.e., maximize R_{369}) at a given FWHM, we find that $\Gamma_{369} = 2\pi \times (\mathrm{FWHM})/\sqrt{3}$ and $\Omega = 2\pi \times (\mathrm{FWHM})/\sqrt{3\beta}$, which gives $R_{369} = 2\pi \times (\mathrm{FWHM})/\sqrt{27}$ when the microwave frequency is resonant with the hyperfine transition. The time to optically pump the ions from the upper clock state to the lower state is $\sqrt{3}\beta/[2\pi \times (\mathrm{FWHM})]$. Thus, the 1-to-1 transition can be used to interrogate the clock transition much faster than the 1-to-0 transition in a continuous mode. However, in the continuous mode, many fewer photons are scattered per microwave photon absorbed compared to a "pulsed mode" of operation, where the microwave radiation and the 369 nm laser light are sequentially applied. In this paper, the 1-to-1 transition and the 1-to-0 transition are used in the continuous mode and the pulsed mode, respectively. A more thorough discussion of the pulsed and continuous modes is found in Ref. [23]. For a chosen linewidth in the continuous mode, the 369 nm laser power and the microwave power are set for maximum R_{369}. In practice, this is achieved by setting the appropriate laser power while applying a large microwave power to give a maximum scattering rate at that laser power, $\frac{1}{2}\Gamma_{369}$. Then, the microwave power is reduced by 2/3 such that $R_{369} = \frac{2}{3}\frac{1}{2}\Gamma_{369} = 2\pi \times (\mathrm{FWHM})/\sqrt{27}$. A sample of the microwave linewidths from 2 Hz up to 276 Hz is shown in Fig. 1(d). The 369 nm power increases from a few nW to hundreds

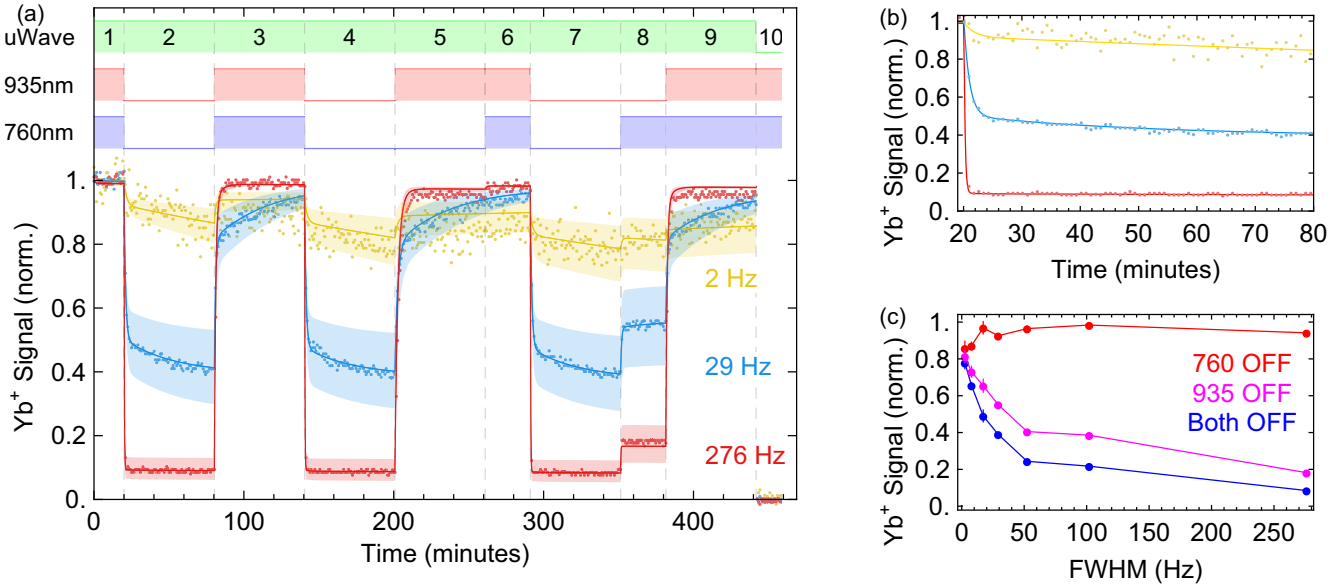

FIG. 2. (a) Normalized Yb fluorescence signal for different microwave linewidths. The data (circular markers) are compared to the simulations (solid lines) to obtain the best free parameters. The data are contain well within a ±20% level of the free-parameter values (shaded regions). The state (on or off) of the microwave radiation, the 935 nm laser, and the 760 nm laser are represented by the respective green-, red-, and blue-shaded regions at the top of the plot. The dashed lines divide the experiment into small segments labeled by numbers from 1 to 10. The background level is determined by turning off the microwave radiation. Data points represent the normalized photomultiplier counts with a 0.1 s gate. (b) The Yb signal of segment 2 in plot (a). (c) Comparing the fractional Yb signals at varying linewidths of the microwave transition. Data show the fractional signals without the 760 nm laser at the end of segment 5 (red markers), without the 935 nm laser at the end of segment 8 (magenta markers), and without both of the lasers at the end of segment 7 (blue markers). Data points and error bars represent the means and standard deviations of 100 normalized photomultiplier counts with a 0.1 s gate.

nW as the microwave linewidth is increased from a few Hz to a few-hundred Hz.

IV. POPULATION DYNAMICS AND THE MOLECULAR ION FORMATION

A. Population dynamics

To understand the molecular formation mechanism, we optically excite the ^{171}Yb$^+$ ions and observe the Yb$^+$ ion signal under different excitation scenarios [Fig. 2(a)]. We perform experiments for different microwave linewidths (2, 29, and 276 Hz) using the 1-to-1 transition. To monitor the ion signal, the ^{171}Yb$^+$ ions are continuously pumped from the S state to the P state by the 369 nm laser. The Yb$^+$ ion signal is detected by collecting the 369 nm photons spontaneously emitted from the P state to S state. Here, the background level is determined by turning off the microwave radiation. The microwave-off signal yields a similar photon count as detuning the 369 nm laser away from the 1-to-1 transition. Since the spontaneous emission occurs extremely fast ($\sim 10^8$ s^{-1}) compared to the optical pumping rate (10^2 s^{-1} or less), the steady-state fractional population of the P state is nearly zero. The Yb$^+$ ion signal normalized to unity reflects the fraction of the population in the S state.

To validate that molecular ions are formed from the F-state ions, we compare data to the numerical simulation of Eq. (1). Here, R_{DF}, R_F, R_{FM}, R_M, and R_{760} are free parameters of the rate equation. We first focus on segment 2 of Fig. 2(a), which is enlarged in Fig. 2(b). As the 760 nm and 935 nm lasers are turned off, the Yb fluorescence signal will decay. To roughly estimate the free parameters, we use the 29 Hz linewidth data since this data set has an obvious double-decay feature. Here, the laser powers are $P_{369\,\mathrm{nm}} = 127$ nW, $P_{760\,\mathrm{nm}} = 0.45$ mW, and $P_{935\,\mathrm{nm}} = 0.52$ mW. The fast decay occurring within the first few minutes is due the F-state trapping [18–20]. The ratio of R_F and R_{DF} determines the normalized ion signal after the fast decay. The sum $R_F + R_{DF}$ determines the ion-signal decay rate. We attribute the slow decay on an hour timescale to the YbH$^+$ formation. The ratio of R_M and R_{FM} determines the ion-signal steady-state value, and the sum $R_M + R_{FM}$ determines the ion-signal decay rate. Starting from this initial estimation, we perform the simulations iteratively to determine the free parameters. The free parameters are determined by minimizing the root-mean-square error (RMSE) between the data and the simulation. We estimate that $R_{DF} \approx 1.03$, $R_F \approx 8.64 \times 10^{-3}$, $R_{760} \approx 10 \times 10^{-3}$, $R_{FM} \approx 0.22 \times 10^{-3}$, and $R_M \approx 0.43 \times 10^{-3}$ s^{-1}. The data are well contained within a ±20% level of the free-parameter values, as shown by the shaded region of Fig. 2(a). R_{760} is determined using segment 8 in Fig. 2(a). Once the free parameters are determined for the 29 Hz linewidth data, we use the same free parameters R_{DF}, R_F, R_{760}, and R_{FM} for the 2 and 276 Hz simulations. Since the molecular ions can be disassociated by the 369 nm light, we assume that an effective disassociation rate R_M is proportional to R_{369}, which is proportional to the 369 nm optical power. Overall, the data agree well with the numerical simulation. This result suggests that the ^{171}Yb$^+$ molecular ions are formed largely from the F-state ions since molecular formation from the D state is not included in the numerical model. Previous work

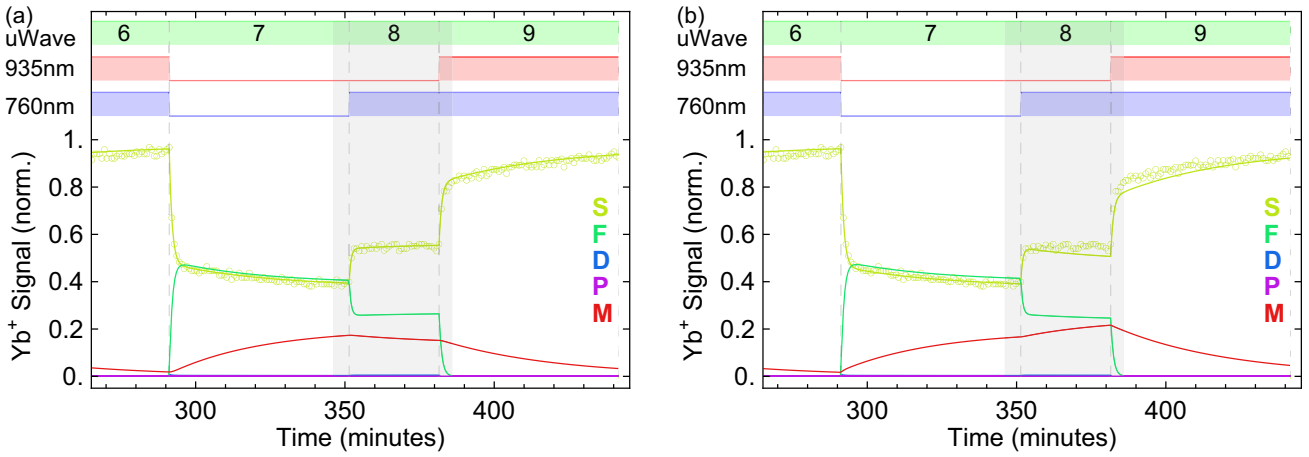

FIG. 3. Comparison of (a) the $F \rightarrow \mathrm{YbH}^+$ simulation model and (b) the $D \rightarrow \mathrm{YbH}^+$ simulation model. The data is the 29 Hz data from Fig. 2(a). The simulated populations of the different energy states are represented by different colors. The colored letters represent the corresponding YbH^+, P, D, F, and S states. The Yb signal (norm.) is normalized to unity. Data points represent the normalized photomultiplier counts with a 0.1 s gate.

has suggested that the molecular ions can be formed from the D or F states through an interaction with hydrogen gas [22]. This is discussed in more detail below.

Moreover, the data indicate that the 760 nm has little effect on the 369 nm fluorescence signal [Fig. 2(c)]. The Yb signal does not show a significant reduction under the absence of the 760 nm laser. This indicates that the $^{171}\mathrm{Yb}^+$ ion clock may be operated in a continuous mode without the 760 nm laser. The 935 nm laser alone can maintain the Yb signal at a sufficient level. When the microwave linewidth is less than a few Hz, the 369 nm fluorescence signal does not reduce much as we turn off both the 935 and 760 nm lasers. The 369 nm fluorescence signal only reduces by 20%. However, it is important to note that these behaviors depend on the exact composition of the gases within the vacuum package. If the decay rate out of the F-state back to the S-state R_F is too slow, an F-state clearing laser may be required, and R_F depends on the background gas composition. Since our vacuum package is permanently sealed, the exact composition in this package is not known.

B. Comparison of $D \rightarrow \mathrm{YbH}^+$ and $F \rightarrow \mathrm{YbH}^+$ simulations

To further verify that the molecular ions are formed primarily from the F-state ions, we perform a $D \rightarrow \mathrm{YbH}^+$ simulation where YbH^+ ions are formed only from ions in the D state. In the $D \rightarrow \mathrm{YbH}^+$ simulation, we used the same free parameters obtained from the $F \rightarrow \mathrm{YbH}^+$ simulation [Fig. 2(a)], except that R_{FM} is set to zero. The rate of forming YbH^+ from D-state ions is $R_{DM} \sim 25 \times 10^{-3}\ \mathrm{s}^{-1}$. When the $D \rightarrow \mathrm{YbH}^+$ simulation to the $F \rightarrow \mathrm{YbH}^+$ simulation is compared, they both agree well with the 29 Hz linewidth data through segment 7 in Fig. 3. However, the $D \rightarrow \mathrm{YbH}^+$ simulation does not agree with the data at segments 8 and 9 [Fig. 3(b)]. In segment 8, the 760 nm laser is turned on after blocking both the 760 and 935 nm lasers for a long period. The $D \rightarrow \mathrm{YbH}^+$ model predicts that the 369 nm fluorescence signal will increase rapidly right after the 760 nm is turned on as ions are cleared out of the F state. The ions then will be transferred quickly into the D state [Fig. 1(c)]. From the D state, the ions would form the YbH^+ molecular ions. As a result, the Yb^+ signal should slowly decrease after an initial jump. However, the Yb^+ signal does not decrease like the $D \rightarrow \mathrm{YbH}^+$ model predicts. The Yb^+ signal instead slightly increases, which is more consistent with the $F \rightarrow \mathrm{YbH}^+$ simulation. Since the 760 nm laser clears F-state ions, the molecular formation from F-state ions will be reduced. As a result, the ion signal increases when YbH^+ molecules are disassociated back to Yb^+ ions.

In a combined model, we can allow both $F \rightarrow \mathrm{YbH}^+$ and $D \rightarrow \mathrm{YbH}^+$ to occur simultaneously. When R_{DM} is reduced to $\sim 5 \times 10^{-3}\ \mathrm{s}^{-1}$ and R_{FM} is $\sim 0.18 \times 10^{-3}\ \mathrm{s}^{-1}$, the combined model can still match the data. When $R_{DM} > 5 \times 10^{-3}\ \mathrm{s}^{-1}$, the combined model shows a similar problem as the $D \rightarrow \mathrm{YbH}^+$ model, as we discussed above [Fig. 3(b)]. If we calculate the rate of molecular formation with the combined model from the D state and F state, we find the maximum value of $n_D R_{DM} = 20 \times 10^{-6}\ \mathrm{s}^{-1}$ and the minimum value of $n_F R_{FM} = 84 \times 10^{-6}\ \mathrm{s}^{-1}$. This demonstrates that the dominant process for YbH^+ is from the F state in our system, and the $D \rightarrow \mathrm{YbH}^+$ contribution can be largely ignored when modeling to limit the free parameters.

C. Disassociating YbH^+ molecules

Previous studies have shown that the YbH^+ molecular ions can be disassociated using 369 nm light tuned to particular resonant wavelengths [14,21,22]. The disassociation wavelengths occur at 369.48, 369.44, 369.20, and 368.95 nm. We perform dissociation spectroscopy to detect YbH^+ molecules using a laser tuned to the 369.48 nm wavelength. For this experiment, two 369 nm lasers are used. First, the ions are exposed to 50–76 μW of light to dissociate the molecules. Then, the second laser is applied on resonance with the 1-to-1 transition (at 369.5251 nm) to monitor the ion signal after the disassociation period. The 760 nm laser is on while the 935 nm laser is blocked. If the molecular disassociation occurs, the number of Yb^+ ions will increase. As a result, the ion signal will increase.

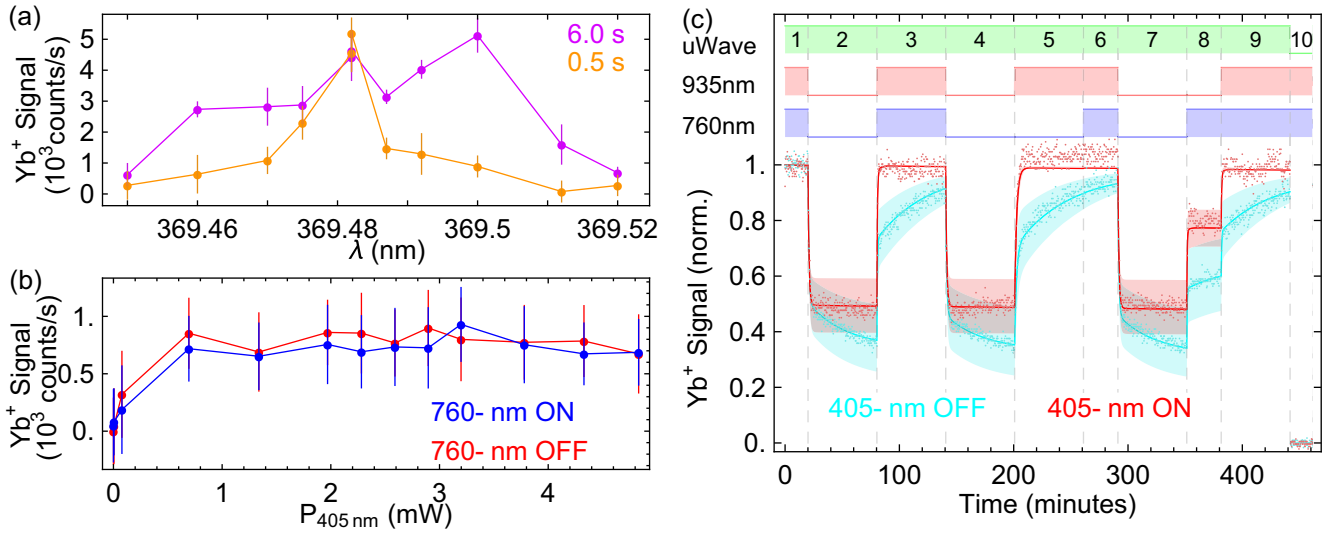

FIG. 4. (a) Plot of molecular dissociation using the 369 nm light. The colored numbers indicate the total time that the ions are exposed to the 369 nm light. For a 0.5 s disassociation, the Yb signal peaks at 369.482 nm. The molecular ions can be disassociated even with off-resonant light if the molecular ions are exposed to the 369 nm light longer. Here the power of the disassociation laser is about 50–76 μW. Data points and error bars represent the means and the standard deviations of 5 photomultiplier counts with a 0.1 s gate. (b) Molecular ion disassociation with 405 nm. The molecular ions are exposed to the 405 nm light for 10 s. The beam-waist diameter is about 1.4 mm. The red (blue) points are when the 760 nm laser is off (on). Data points and error bars represent the means and standard deviations of 90 photomultiplier counts with a 0.1 s gate. (c) Fractional Yb signal at a 30 Hz linewidth with and without the 405 nm disassociation laser. The 405 nm laser power is ~2.7 mW. When the 405 nm light is on, the disassociation rate R_M is about 20 times higher than the molecular formation rate R_{FM}.

As we scan the 369 nm laser across the 369.48 nm disassociation wavelength, the ion signal shows a resonance peak at 369.482 nm [Fig. 4(a)]. This is an indication of the YbH$^+$ disassociation. This observation is consistent with the earlier studies [14,21,22]. When the disassociation time is prolonged to 6 s, the disassociation linewidth is broadened. With 0.5 s of disassociation time, the resonance peak has a FWHM of about 15 pm (33 GHz). The FWHM is broadened to about 100 pm for the 6 s disassociation. This indicates that the molecular ions can be disassociated using light off-resonant from the molecular transition.

Since the Yb$^+$ signal is collected using the 369 nm photons emitted from trapped ions, using 369 nm light for the molecular disassociation will increase background noise. For a Yb$^+$ ion clock, a high background level will degrade the clock stability. For this reason, we demonstrate that 405 nm light can disassociate YbH$^+$. Using a free-running edge-emitting diode laser, we apply 405 nm light to the trapped ions for 10 s with varying power with the 935 nm laser off. The ion signal increases to a steady level after the 405 nm laser power reaches above a 1 mW level [Fig. 4(b)]. We also compare the disassociation process with and without the 760 nm laser. If the 405 nm light could clear the F state, the Yb$^+$ signal with the 760 nm laser should be higher than that without the 760 nm laser. Since the results with and without the 760 nm are comparable, the Yb$^+$ signal increases mainly due to the YbH$^+$ disassociation.

We also compare the Yb$^+$ signal with and without the 405 nm laser using the same procedure as in Fig. 2. We will first focus on segment 2 of Fig. 4(c), where both the 760 and 935 nm lasers are blocked, to illustrate the effect of the 405 nm laser. When the 405 nm laser is absent, the trapped ions will quickly fall into the F state [18–20] and then slowly form YbH$^+$, as discussed in the previous section. The Yb$^+$ signal without the 405 nm laser shows the double-decay time constants as expected. On the other hand, the 405 nm laser will significantly increase the YbH$^+$ dissociation rate. When the YbH$^+$ disassociation rate is much faster than the YbH$^+$ formation rate, the YbH$^+$ population is negligible. Under the presence of high 405 nm laser power, the trapped ions will quickly fall into the F state with a negligible YbH$^+$ population. The data show that the Yb$^+$ signal quickly decays to a steady state due to the F-state trapping. Overall, the data show a good agreement with the numerical simulation of Eq. (1). We estimate that $R_{DF} \approx 1.08$, $R_F \approx 9.6 \times 10^{-3}$, $R_{760} \approx 29 \times 10^{-3}$, $R_{FM} \approx 0.32 \times 10^{-3}$, and $R_M \approx 0.36 \times 10^{-3}$ s^{-1}. Here we compare the data without the 405 nm laser to the theoretical model to obtain the free parameters [24]. We use the same parameters to simulate the population dynamics under the presence of the 405 nm laser. To include the molecular dissociation effect of the 405 nm laser, we simply change the molecular disassociation rate R_M. The data with the 405 nm laser agree well with the numerical simulation when the R_M rate is about 20 times larger than the molecular formation rate R_{FM}. The normalized Yb$^+$ signal with 405 nm laser rises above unity in segments 5 and 6 due to background fluctuations. The free-running 405 nm laser diode is not stable, and its laser-power fluctuations can perturb the photon count of the photomultiplier tube.

D. Pulsed-mode operation

Since a ytterbium ion clock is often operated in the pulsed mode, we will briefly discuss the population dynamics under pulsed-mode operation. In the pulsed mode, either a single Rabi or two Ramsey microwave pulses are applied to the ions,

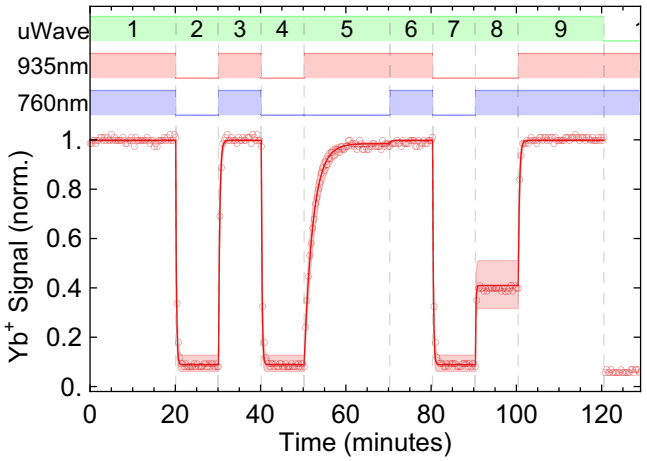

FIG. 5. Normalized Yb fluorescence signal in pulsed-mode operation (1.45 s of microwave and 0.25 s of 369 nm light). The 369 nm power is ∼10 μW, which yields an optical pumping time of 23 ms. The data are contain well within a ±20% level of the free-parameter values, as shown by the shaded region. Each fluorescence signal data point is collected in the first 10 ms after the light is turned on. The background level is determined by detuning the 369 nm laser away from the 1-to-0 transition.

followed by a 369 nm light pulse. We typically apply a single pulse, which transfers ions from the $|^2S_{1/2}, F = 0\rangle$ state to the $|^2S_{1/2}, F = 1\rangle$ state, and fluorescence collected during the 369 nm light pulse determines the relative populations of the two states. Since the 369 nm light is off during the microwave interrogation, the pulsed mode does not suffer the light-shift problem as in the continuous mode of operation. In the pulsed mode, we apply 10 μW of 369 nm power, which optically pumps the ions back to the $|^2S_{1/2}, F = 0\rangle$ with a time constant of ∼23 ms. Figure 5 shows the Yb^+ signal in the pulsed-mode operation (1.45 s of microwave and 0.25 s of 369 nm light). Rather than a full multistate model, we implement a simplified two-level model that includes only the S state and the F state, as described in Ref. [20]. Since the 10 μW of 369 nm light can disassociate YbH^+ quickly, the YbH^+ population is not considered. With the rapid spontaneous decay of the P state, the population of the P state is nearly zero. Also, the decay rate of the D state is much faster than those rates associated with going into and out of the F state, so the short timescale dynamics of the D state is neglected, and the D-state population is given as a fraction α_D of the S state. In this way, we only consider the steady-state populations after each pulse, and the long-timescale pulsed-mode dynamics is given by modifying Eq. (1) as

$$\begin{aligned} \dot{n}_S &= -\alpha_D r_{DF} n_S + (r_F + r_{760} + r_{FM}) n_F, \\ \dot{n}_F &= -(r_F + r_{760} + r_{FM}) n_F + \alpha_D r_{DF} n_S. \end{aligned} \tag{3}$$

Since α_D is the fraction of the S-state population in the D state, it will depend on the ratio of the microwave pulse length to the 369 nm laser pulse length, the 369 nm laser power, and the 935 nm laser power, which clears ions out of the D state. Adding the parameter α_D into Eq. (3) is equivalent to adjusting the effective rate going from the S state to the F state due to the two-level simplification. Since ions in the D and P states and the YbH^+ molecules also decay into the S state during the pulsed-mode operation, the effective rates from the F state to S state have to be adjusted to compensate for these ignored states in the two-level model. Here r_{DF}, r_F, r_{FM}, and r_{760} are the effective rates from the F state to S state, which corresponds to R_{DF}, R_F, R_{FM}, and R_{760} in the continuous-mode model, respectively. The data agree well with the numerical simulation of Eq. (3) when $r_F = 7.8 \times 10^{-3}\,\mathrm{s}^{-1}$, $r_{760} = 49 \times 10^{-3}\,\mathrm{s}^{-1}$, $r_{FM} = 0.22 \times 10^{-3}\,\mathrm{s}^{-1}$, $r_{DF} = 1.19\,\mathrm{s}^{-1}$, and

$$\alpha_D = \begin{cases} 104 \times 10^{-6}, & 935\text{ nm ON}, \\ 69 \times 10^{-3}, & 935\text{ nm OFF}. \end{cases}$$

Here, the r_F, r_{760}, and α_D parameters are obtained by minimizing the RMSE between the data and the simulation. The rate constants r_{FM} and r_{DF} cannot be determined from the data because they are not independent of r_F and α_D, respectively, in the model, and they are set equal to R_{FM} and R_{DF} from the continuous-mode results. The data are well contained within the ±20% level of the free parameters, as shown by the shaded region of Fig. 5. Overall, the parameters are similar to those found for the continuous-mode data. The effective pumping rate R_{760} of the pulsed-mode data is about three times higher than that of the continuous-mode results. This difference is an effect of the two-level simplification, as discussed above. We note that to obtain a more precise description of the pulsed-mode dynamics, a simulation including all energy levels should be used while observing the fluorescence decay for each pulse of the 369 nm laser. Since this type of simulation requires a small integration step ($<10^{-2}$ s), it is not ideal to simulate a few hours of experimental data. Finally, while the vacuum package used in this work had little F-state trapping without the use of the 760 nm laser, other sealed vacuum packages required the 760 nm laser to avoid significant F-state populations. The F-state trapping that we assume depends on the exact gas background in the package, which depends on the details of the preparation of the vacuum package and how long since it has been sealed.

V. CONCLUSION

In conclusion, we have demonstrated that the formation of YbH^+ molecular ions occurs when the ytterbium ions are primarily in the F state. The experimental data show good agreement with the theoretical model that YbH^+ molecules are dominantly formed from the F state. Our numerical simulation indicates that YbH^+ molecules may be formed from the D-state ions; however, the $D \rightarrow YbH^+$ rate is much smaller than the $D \rightarrow F$ rate, and thus the large F-state population gives rise to YbH^+ being formed mainly from the F state in our system. Our study indicates that the 760 nm has little effect on Yb^+ ions when the 369 nm power is low. Since 935 nm light can clear ions out of the D- state, it can stop ions going into the F state from the D state. If the ions do not populate the F state, they will likely not form YbH^+ molecules. Therefore, it is possible to run a Yb^+ atomic clock in a continuous mode using only a 369 and 935 nm laser. We also demonstrate that YbH^+ molecules can be disassociated using off-resonant 405 nm light. With the permanently sealed vacuum packages used in our work, the exact composition of the gas background can change from package to package,

giving different rates for R_F, R_{DF}, R_M, and R_{FM}. Once these rates are known, our model can determine how to minimize the number of molecular ions and Yb ions in the F state.

ACKNOWLEDGMENTS

The authors would like to thank Jeff Hunker for assembling various parts of the apparatus and John D. Prestage and Sang Chung for fabricating the vacuum package. This research was developed with funding from the Defense Advanced Research Projects Agency (DARPA). The views, opinions, and/or findings expressed are those of the authors and should not be interpreted as representing the official views or policies of the Department of Defense or the US Government. Sandia National Laboratories is a multimission laboratory managed and operated by National Technology and Engineering Solutions of Sandia, LLC, a wholly owned subsidiary of Honeywell International, Inc., for the US Department of Energy's National Nuclear Security Administration under Contract No. DE-NA0003525.

[1] J. Sebby-Strabley, C. Fertig, R. Compton, K. Salit, K. Nelson, T. Stark, C. Langness, and R. Livingston, Design innovations towards miniaturized GPS-quality clocks, in *2016 IEEE International Frequency Control Symposium (IFCS)* (IEEE, 2016), pp. 1–6.

[2] X. Liu, E. Ivanov, V. I. Yudin, J. Kitching, and E. A. Donley, Low-Drift Coherent Population Trapping Clock Based on Laser-Cooled Atoms and High-Coherence Excitation Fields, Phys. Rev. Appl. **8**, 054001 (2017).

[3] D. R. Scherer, R. Lutwak, M. Mescher, R. Stoner, B. Timmons, F. Rogomentich, G. Tepolt, S. Mahnkopf, J. Noble, S. Chang, and D. Taylor, Progress on a miniature cold-atom frequency standard, arXiv:1411.5006.

[4] S. Knappe, V. Shah, P. D. Schwindt, L. Hollberg, J. Kitching, L.A. Liew, and J. Moreland, A microfabricated atomic clock, Appl. Phys. Lett. **85**, 1460 (2004).

[5] R. Lutwak, A. Rashed, M. Varghese, G. Tepolt, J. Leblanc, M. Mescher, D. K. Serkland, and G. M. Peake, The miniature atomic clock-pre-production results, in *2007 IEEE International Frequency Control Symposium Joint with the 21st European Frequency and Time Forum* (IEEE, 2007), pp. 1327–1333.

[6] L. Maleki, A. A. Savchenkov, V. S. Ilchenko, W. Liang, D. Eliyahu, A. B. Matsko, D. Seidel, N. P. Wells, J. C. Camparo, and B. Jaduszliwer, All-optical integrated rubidium atomic clock, in *Proceedings 2011 Joint Conference of the IEEE International Frequency Control and the European Frequency and Time Forum (FCS)*, (IEEE, 2011), pp. 1–5.

[7] G. Phelps, N. Lemke, C. Erickson, J. Burke, and K. Martin, Compact optical clock with 5×10^{-13} instability at 1 s, J. Inst. Navig. **65**, 49 (2018).

[8] J. D. Prestage and G. L. Weaver, Atomic clocks and oscillators for deep-space navigation and radio science, Proc. IEEE **95**, 2235 (2007).

[9] Y.-Y. Jau, H. Partner, P. D. Schwindt, J. D. Prestage, J. R. Kellogg, and N. Yu, Low-power, miniature ^{171}Yb ion clock using an ultra-small vacuum package, Appl. Phys. Lett. **101**, 253518 (2012).

[10] P. D. Schwindt, Y.-Y. Jau, H. Partner, A. Casias, A. R. Wagner, M. Moorman, R. P. Manginell, J. R. Kellogg, and J. D. Prestage, A highly miniaturized vacuum package for a trapped ion atomic clock, Rev. Sci. Instrum. **87**, 053112 (2016).

[11] P. D. Schwindt, Y.-Y. Jau, H. L. Partner, D. K. Serkland, A. Ison, A. McCants, E. Winrow, J. Prestage, J. Kellogg, N. Yu, C. D. Boschen *et al.*, Miniature trapped-ion frequency standard with ^{171}Yb$^+$, in *2015 Joint Conference of the IEEE International Frequency Control Symposium and the European Frequency and Time Forum (FCS)* (IEEE, 2015), pp. 752–757.

[12] H. Lehmitz, J. Hattendorf-Ledwoch, R. Blatt, and H. Harde, Population Trapping in Excited Yb Ions, Phys. Rev. Lett. **62**, 2108 (1989).

[13] H. A. Klein, A. S. Bell, G. P. Barwood, and P. Gill, Laser cooling of trapped Yb$^+$, Appl. Phys. B **50**, 13 (1990).

[14] A. Bauch, D. Schnier, and C. Tamm, Collisional population trapping and optical deexcitation of ytterbium ions in a radio-frequency trap, J. Mod. Opt. **39**, 389 (1992).

[15] C. Tamm, A tunable light source in the 370 nm range based on an optically stabilized, frequency-doubled semiconductor laser, Appl. Phys. B **56**, 295 (1993).

[16] A. Bell, P. Gill, H. Klein, A. Levick, and W. Rowley, Precision measurement of the $^2f_{7/2} - {}^2d_{5/2}$ 2.43 μm interval in trapped ^{172}Yb$^+$, J. Mod. Opt. **39**, 381 (1992).

[17] D. J. Seidel and L. Maleki, Efficient quenching of population trapping in excited Yb$^+$, Phys. Rev. A **51**, R2699(R) (1995).

[18] N. Yu and L. Maleki, Lifetime measurements of the $4f^{14}5d$ metastable states in single ytterbium ions, Phys. Rev. A **61**, 022507 (2000).

[19] M. M. Schauer, J. R. Danielson, A.-T. Nguyen, L.-B. Wang, X. Zhao, and J. R. Torgerson, Collisional population transfer in trapped Yb$^+$ions, Phys. Rev. A **79**, 062705 (2009).

[20] Y.-Y. Jau, J. Hunker, and P. Schwindt, F-state quenching with Ch_4 for buffer-gas cooled ^{171}Yb$^+$ frequency standard, AIP Adv. **5**, 117209 (2015).

[21] K. Sugiyama and J. Yoda, Disappearance of Yb$^+$ in excited states from rf trap by background gases, Jpn. J. Appl. Phys. **34**, L584 (1995).

[22] K. Sugiyama and J. Yoda, Production of YbH$^+$ by chemical reaction of Yb$^+$ in excited states with H_2 gas, Phys. Rev. A **55**, R10(R) (1997).

[23] P. D. Schwindt, T. M. Hoang, Y.-Y. Jau, and R. Overstreet, Operating a ^{171}Yb$^+$ microwave ion clock in a continuous mode, in *2018 IEEE International Frequency Control Symposium (IFCS)* (IEEE, 2018), pp. 1–4.

[24] It is worth noting that these rate constants are not solely the intrinsic properties of the trapped ions, but depend on external conditions (e.g., vacuum conditions). The data of Fig. 2(a) and the data of Fig. 4(c) were taken at different times (i.e., different vacuum conditions) and with different laser-power settings. Here, $P_{369\,\mathrm{nm}} = 64$ nW, $P_{760\,\mathrm{nm}} = 0.59$ mW, and $P_{935\,\mathrm{nm}} = 0.51$ mW. Therefore, the rate constants R_{760} and R_M should be different from the rate constants obtained in Fig. 2(a).